TECHNICAL UNIVERSITY OF CLUJ-NAPOCA

ACTA TECHNICA NAPOCENSIS

Series: Applied Mathematics, Mechanics, and Engineering
Vol. 60, Issue I, March, 2017

COMPUTER AIDED PARAMETRIC DESIGN OF HYDRAULIC GEAR PUMPS

Ionuţ Gabriel GHIONEA, Nicolae IONESCU, Adrian GHIONEA, Saša ĆUKOVIĆ, Sergiu TONOIU, Mădălin CATANĂ, Iqbal JAMSHED

Abstract: *This paper addresses methodological and applied issues to design spur gear pumps. Based on the requirements raised by a Romanian production partner, the overall objective of this research is to identify several design alternatives and to propose improved construction solutions, which are strongly backed by mathematical validation and finite element simulation. The parametric design is simulated using finite element method to prove the concept for a wider range of flow rates. Using tools like CATIA and Visual Basic programming language, the proposed strategy presents the results summarizing the values of maximum stress, deformation and the percentage calculation error for each constructive solution.*
Key words: *FEM analysis, Spur gears pump, Parametric modelling, Pump flow.*

1. INTRODUCTION

Spur gear pumps have a wide range of applications due to a special constructive simplicity, low cost and operational safety. There is a wide variety of such pumps, which can be classified by: pressure level (low, medium and high) gear type (external or internal, straight, bevel or V-shaped), tooth profile (involute or cycloid), pump capacity (constant or adjustable), number of rotors (bi- or multirotor).

Currently, many research papers aimed at developing hydraulic gear pumps on modern principles: increasing the operating pressures [1], [2], extending the production range [3], [4] improving operational efficiency [2], [5] reduction of the pressure variations, of the dynamic loads [3], [6], [7], weight [4], etc.

Through parametric design, the authors have achieved and proposed the range of production, through size variation of certain components and their modular assembly, resulting flow rates of 2 to 22.52 l/min at a rotary speed of 3000 rev/min. For the alternative solution producing the smaller flow rates, the pump can be considered to be part of group 0 (micropumps, 1 cm^3/rev) with reduced overall dimensions.

2. PARAMETRIC DESIGN OF THE PUMP

From among a large variety of CAD systems considered in this paper for the proposed product modelling and simulation using the finite element method FEM, the authors selected the CATIA v5 software, which can perform the pump complex parameterization. Geometrical 3D modelling of components is generally based on working drawings provided by a Romanian pumps manufacturer and by measuring of the real parts in the faculty calibration laboratory. The design of the pump assembly depends on the modelling accuracy of the two gears according to the flow rate to be transmitted, the distance between shaft axes and the size of the pump body pockets. Teeth flanks are defined by the involute profile shape and by the shape of toothing line, the profile and flank line equations are based on parameterization. The pump gear is designed with corrected toothing [8].

For the representation of the gear, body and flanks, the following steps must be considered: draw the involute tooth profile, multiply it on the

circumference of the gear, extrude the entire toothing contour on the specified width and determine the assembly and driving surfaces, according to the methodology presented in detail in papers [2], [9] and others. By applying the specific techniques of the parametric modelling, it was obtained the correct profile for the cylindrical spur gears and also subsequently the pump's gearing, each gear having 12 teeth. The gears are integral with the support and driving elements. Modelling the other components of the pump was done according to the dimensions derived from the working drawings and by measuring of the real parts in the faculty calibration laboratory. Throughout modelling, the authors aimed at identifying the parameters that are part of the established formulas for parametric design.

The authors considered many parameters: the diameter and length of each shaft, the distance between their axes, the driving and supporting elements, the support holes diameters for the gears shafts, the diameters of the bores in which the gears are positioned, mounted and rotating, the distance between axes of these holes, depth of the pockets in which are installed the compensator and gears (driving & driven gears) [9], [10]. The compensator has been created through parametric design so that its profile's nominal diameters are equal to the diameters of the gear head circle and thus equal to diameters of the bores made in the pump body. The body holes diameters are equal to the diameters of the gears shafts and the distance between the axes of these holes is equal to the distance between the shafts axes. The radii of the lateral openings is parameterized on discrete values, to let the hydraulic fluid pass into the holes provided to ensure lubrication of the gears shafts bearings provided in the pump body and cover [10]. Such conditions are set for all the pump components, resulting various sets of formulas, conditions and constraints with an important role in parameterization. The real pump and the result of modeling, a 3D solid model (isometric exploded view) are shown in Fig. 1.

Once geometrical modelling is completed, the parametric design of pumps proceeds under certain functional and dimensional conditions [11]. Parametric design is based on the pump's flow rate which it can convey and is in direct connection to one of the basic characteristics of hydrostatic pumps, called geometrical volume, expressed through the Eq. 1 [12]:

$$V_g = 2 \cdot z \cdot b \cdot A \cdot 10^{-3} \text{ [cm}^3\text{/rot]} \quad (1)$$

where: z – the number of teeth on each gear, b – gear width, in mm, A – area of the space profile between two consecutive teeth, in cm^2. This area is geometrically determined, its value being dependent on the specific parameters of gears: modulus, number of teeth, angle of gearing, correction coefficient.

The teeth space profile area decreases with the increase of teeth number, and determines the inner overall size of the pump. Knowing the area, we calculate the volume of interspace between two teeth, then the geometric volume V_g of the pump. The pump flow rate is defined by Eq. 2, as follows:

$$Q_p = \frac{V_g \cdot n}{10^3} \cdot \eta_v \text{, [l/min]} \quad (2)$$

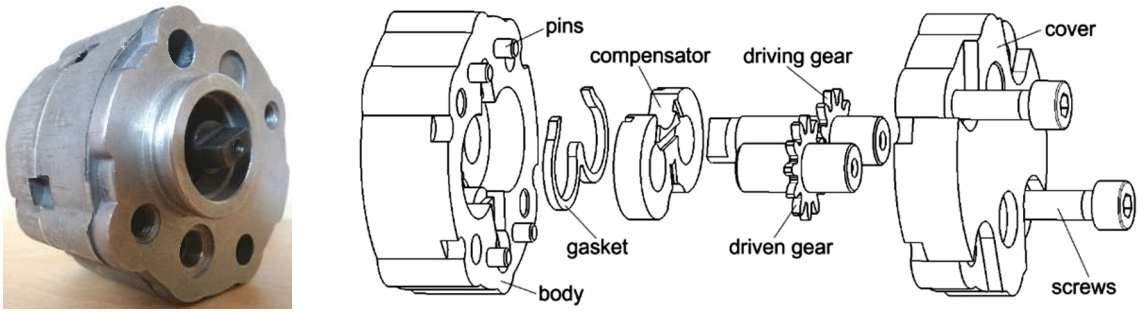

a. b.

Fig. 1. a. Real spur gear pump and b. 3D CAD representation – exploded view with all its components

where: n - rotational speed of the driving shaft, in rot/min, and η_v - the volumetric efficiency, in %.

In the current case, n=3000 rot/min is the nominal rotational speed (min. n_{min}=700 rot/min and max. n_{max}=5000 rot/min); according to the producer specifications, η_v =93%, according to [10], [11]. The value of this parameter for the standard pump in Fig. 1 is 1.2 cm^3/rev. The aim is to increase geometric volume without changing external size and shape of the stock parts used in the processing of the pump body and cover. This would lead to an increase in the pump flow rate without being necessary to select the next pump in the series, which differs in the size of its components, a solution that would lead to significant additional costs. Maintaining the standard constructive pump configuration can also be achieved by certain existing functional and constructive constraints, in the plant where it provides hydraulic medium with its characteristic flow rate, i.e. keeping the size and distribution of threaded holes for attaching the cover on the body and of passage holes for attaching pump screws in the given place inside the hydraulic plant. Parametric design of the pump aims to provide the flow rate as required by the manufacturer considering a standard type of pumps, a constructive solution, a series of geometrical volumes, with some parameters defined in Eq. 1, the gearing angle, correction parameters, nominal rotational speed.

Based on the geometrical volumes taken into consideration and geometrical requirements (gears teeth width and compensator width not less than 2.2 mm, and 6 mm, respectively), there can be calculated the parameters which define the teeth width, width of the pump body, depth of holes in the body for gears and compensator and width of the latter. Geometrical parametric models of the body, gears and compensator are automatically re-created based on some relations and one reaction (written in Visual Basic) activated by the change in the flow rate of the pump. The parameters values and their correspondence are shown in Tab. 1. Parametric design of the pump consists in keeping the overall size of the cover and body and changing by relations some body dimensions (width and depth of support holes for gears and compensator), gears size (teeth width and shafts lengths supported by bearings provided in compensator and body) and the compensator width.

Table 1

Values of basic parameters affecting pump flow rate

No.	Pump flow rate Q_p,l/min	Nominal speed n, rot/min	Output η_v, %	Geometrical volume V_g, cm^3	Geometrical area A, cm^2	Teeth widths b, mm	Body width H, mm	Depth of bored holes h, mm	Compensator width l, mm
1	2	3000	82	0.81	0.1474	2.3	25	10	7.7
2	2.53		85	0.99		2.8			7.2
3	3.18		88	1.2		3.4			6.6
4	4.58		90	1.7		4.8	25.5	12	7.2
5	6.05		92	2.19		6.2	30	15	8.8
6	7.30		93	2.62		7.4	32		7.6
7	8.98		94	3.18		9	30		6
8	10.08		95	3.54		10	35	20	10
9	12.23		96	4.25		12			8
10	13.55			4.71		13.3			6.7
11	17.32			6.01		17	40	25	8
12	22.52			7.82		22.1	45	30	7.9

Fig. 2 illustrates two constructive solutions of the same pump obtained by parametric design, as follows: a. for the flow rate Q_p=2 l/min, and b. Q_p=22.52 l/min, respectively. Certain components of the assembly (cover, screws, and pins) were not represented to highlight how the parameterized components are changed.

The two 3D models clearly symbolize the parametric design possibilities of the considered assembly, based on the modification criterion of the user required flow rate. There are shown different widths of the bodies, compensators and

gears, different depths of holes, etc. We considered to vary geometrically the pump inlet and outlet chambers with the aim of increasing the pump flow rate, thus resulting a wider range of pump products. During the 3D modeling phase, the pump's components were modified to fulfill the constraints imposed by the FEM analysis.

Fig. 3 presents two variants of the same type of pump, before and after redesign. The body of the new pump uses only 2 pins, not 4 like the previous solution.

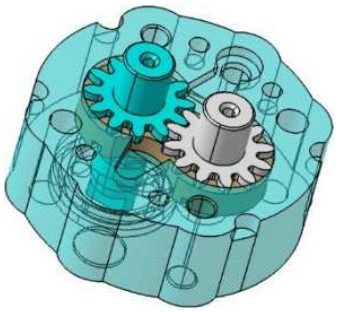

a.

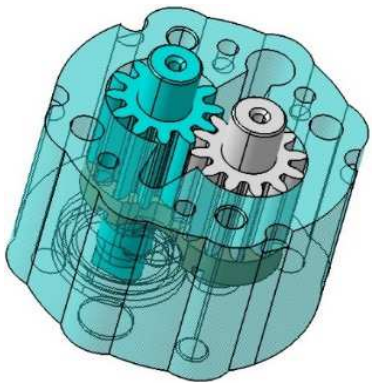

b.

Fig. 2. Parametric model of the pump for two flow rates a. 2 l/min and b. 22.52 l/min

Also, it was changed the position and diameter of the hole from the outlet chamber. The new pump cover has also only 2 pins, instead of 4 met in the previous pump. This modification was imposed by a high stress value located near the pins. In time, a failure crack may appear connecting the outlet chamber, the gasket channel and the screw hole. In the pump cover, the left pocket is used only by the fixture device during machining. The new pump compensator has the gasket channel slightly larger and obtained directly from the casting phase. The previous compensator was contour milled. For the new compensator, a supplementary thin plastic gasket is added to better seal the pump chambers. It also prevents the movement and premature wear of the rubber gasket.

a.

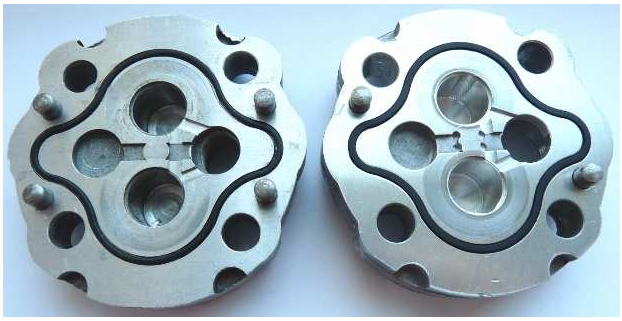

b.

c.

Fig. 3. Two variants of a. pump body, b. cover and c. compensator. In each subfigure, left one shows the old pump solution, while right one corresponds to the new solution, after the whole parameterization process

3. NUMERICAL ANALYSIS OF THE SPUR GEAR LOADS

To determine the behaviour of the external spur gear under the operating conditions, for different constructive alternative solutions, there were determined by mathematical calculation the loads on the pump assembly.

Thus, we followed a specific methodology presented in papers [2] and [16] that aimed mainly to determine the distribution of forces that load the gears, shafts and their bearings. They are mainly affected by the radial components of the elementary forces of pressure on gears and by the gearing forces corresponding to the components of the pressure forces on teeth flanks [2], [6], [7], in each teeth space volume between two adjacent teeth (Fig. 4).

In the addendum area of each tooth, a pressure distribution occurs; its variation between the teeth space and the addendum area is considered very low, so the radial distribution of pressure is considered to be continuous.

The gearing forces oriented along the line of gearing Δ are decomposed on the tangent and radial directions. It is considered that during the nominal regime of the pump, pressure distribution is of parabolic shape [12]. The radial clearance (sliding fit) between gears and their holes in the pump body influences the flow rate and discharge pressure of liquid.

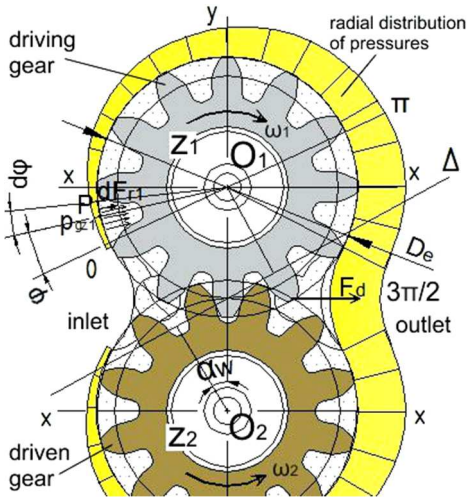

Fig. 4. Radial distribution of pressures

Considering the directions of movement, with the angular speed $\omega_1=\omega_2$ of the two gears, the contact between any teeth (z_{i1}) of the driving gear with the conjugate tooth (z_{i2}) of the driven gear takes place in a point on the gearing line Δ. At that moment, the meshing teeth cause the discharge of liquid from the teeth space into the outlet aperture of the pump. Similarly, the liquid under pressure is discharged from the other gaps as well, with continuous rotation movements. Before the teeth z_{i1} and z_{i2} leave out the meshing area, the next two teeth follow in.

The exertion of pressures generated on the peripheral surfaces of the gears creates a resisting torque, which is counteracted by the engaging of the driving gear. This torque value gives the measure of the pump driving motor power, by means of the Eq. 3:

$$P = \frac{Q_p \cdot p}{6 \cdot \eta_t} = \frac{10^{-3} \cdot V_g \cdot n \cdot p}{6 \cdot \eta_m}, \text{ [kW]} \qquad (3)$$

where the symbols significance are indicated above, while η_t is the total efficiency (%).

The force applied on teeth (and on the liquid, as well) in the x – x direction, as a result of the torque applied on the driving gear (pinion z_1) can be calculated by Eq. 4:

$$F_d = \frac{2 \cdot M_a}{D_w}, \text{ [N]} \qquad (4)$$

where M_a (N·mm) is the torque moment necessary for the driving shaft, while D_w (mm) is the gear rolling diameter. This moment can be calculated with approximations [2] by Eq. 5:

$$M_a = p \cdot m^2 \cdot b \cdot (z_1 + 1), \text{ [N·mm]} \qquad (5)$$

where p is the pressure generated in the pump (in the outlet chamber) during operation (bar), $b=\lambda \cdot m$ – width of gear toothing (mm), λ – width coefficient, m – modulus of toothing (mm) and z_1 – number of teeth of the driving gear.

Values of powers and torques necessary for the pump driving are calculated and presented for each alternative solution in Table 2.

The rolling diameter [11], [12] of the displaced spur gear is given by Eq. 6:

$$D_{w12} = m \cdot (z_{12} + 2 \cdot \xi_{12}), \text{ [mm]} \qquad (6)$$

where ξ is the specific displacement of the gear teeth profile. Thus, the calculation formula of the force applied on the teeth will be Eq. 7:

$$F_d = 2 \cdot p \cdot m \cdot b, \text{ [N]} \qquad (7)$$

and it represents the tangent component of the generated force on the driving gear tooth z_1.

The liquid under pressure filling the teeth space produces stress on the radial direction (Fig. 4) on both gears, with a pressure that varies from a minimal value (atmospheric pressure in the inlet chamber) to the pressure in the outlet chamber estimated as the nominal pressure of the pump.

For an angular variation, $\varphi \in (0 \ldots \pi)$, pressure is rising, while for $\varphi \in (\pi \ldots 3\pi/2)$, pressure constant [10], [16]. Considering a point on the circumference of the driving gear z_1, in the interval $\varphi \in (0 \ldots \pi)$, the pressure generated in the

conveyed liquid to the outlet chamber is $p_{gz1}=p\cdot\varphi/\pi$. This pressure produces a radial elementary force dF_{r1} acting on the outside radius circumference of the gear z_1, corresponding to the angle $d\varphi$. Therefore, the equation of this force is Eq. 8:

$$dF_{r1} = p\cdot\frac{\varphi}{\pi}\cdot b\cdot\frac{D_e}{2}\cdot d\varphi, \text{ [N]} \quad (8)$$

The radial elementary force acting on the interval $\varphi \in (\pi\ldots 3\pi/2)$ is Eq. 9:

$$dF_{r2} = p\cdot b\cdot\frac{D_e}{2}\cdot d\varphi, \text{ [N]} \quad (9)$$

Based on these statements, the total radial force F_{rx} acting in the direction x – x on the gears (z_1 and z_2) is calculated with the relation Eq. 10. here, as an example, the gear angle $\alpha_w=23^0$, the gear has displaced teeth [7], [8]. Here, φ is the rotation angle of the driving gear z_1 and D_{e12} is

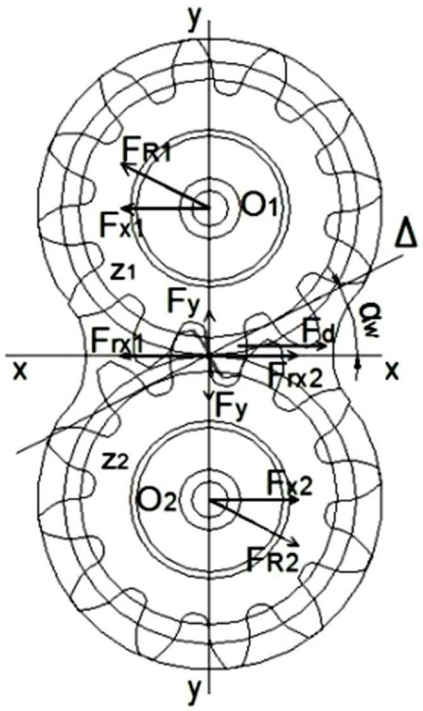

Fig. 5. Forces acting on gears and shafts

$$F_{rx12} = p\cdot b\cdot\frac{D_e}{2\pi}\int_0^{\pi}\varphi\cdot\cos\varphi\cdot d\varphi + p\cdot b\cdot\frac{D_e}{2}\int_{\pi}^{\frac{3}{2}\pi}\varphi\cdot\cos\varphi\cdot d\varphi \approx 0{,}81\cdot p\cdot D_{e12}\cdot b, \text{ [N]} \quad (10)$$

the calculated outer diameter of gears, using the Eq. 11.

$$D_{e12} = m\cdot(z_{12}+2+2\cdot\xi), \text{ [mm]} \quad (11)$$

These two forces F_{rx1}, F_{rx2} (Fig. 5) act on the same directions also in the centers O_1 and O_2 of the two gears, where the resulting forces F_{R1} and F_{R2}, respectively, are considered to act as well.

The radial force acting on the driving shaft z_1 on the direction x – x is determined according to [5] and [7] by aid of the Eq. 12.

For the force applied on the driven shaft z_2, on the same direction, we can use the Eq. 13, $F_{x1} = F_{rx1} - F_d$ and $F_{x2} = F_{rx2} + F_d$.

$$F_{x1} = (0.81\cdot z_1 - 0.38 + 1.62\cdot\xi)\cdot p\cdot m\cdot b, \text{ [N]} \quad (12)$$

$$F_{x2} = (0.81\cdot z_2 + 3.62 + 1.62\cdot\xi)\cdot p\cdot m\cdot b, \text{ [N]} \quad (13)$$

The radial forces calculated using the Eq. 14 acting on the direction y – y on the two meshing gears become null (in conformity with the radial distribution of pressures).

A radial rejecting force is generated as a reaction of teeth in contact, whose value can be determined by Eq. 15.

$$F_y = F_d\cdot tg\,\alpha_w, \text{ [N]} \quad (15)$$

The resulting forces F_{R1}, and F_{R2}, that produce stress on the driving and driven gears bearings are calculated by Eq. 16 and Eq. 17:

$$F_{R1} = p\cdot m\cdot b\sqrt{0.66\cdot z_1^{\,2} + 0.7\cdot z_1 + 0.7}, \text{ [N]} \quad (16)$$

$$F_{R2} = p\cdot m\cdot b\sqrt{0.66 z_2^{\,2} + 3.94 z_2 + 6.4}, \text{ [N]} \quad (17)$$

$$F_{ry12} = p\cdot b\cdot\frac{D_{e12}}{2\cdot\pi}\int_0^{\pi}\varphi\cdot\sin\varphi\cdot d\varphi + p\cdot b\cdot\frac{D_{e12}}{2}\int_{\pi}^{\frac{3}{2}\pi}\sin\varphi\cdot d\varphi = 0, \text{ [N]} \quad (14)$$

To calculate the forces on the basis of the above formulas we considered: p=150 bar, m=2 mm and ξ=0.5 mm; the values of forces F_d, F_{rx1}, F_{rx2}, F_{x1}, F_{x2}, F_y, F_{R1} and F_{R2} are to be calculated (Table 2).

The yield strength is thus defined as the maximum limit of the actual stresses under the safety conditions imposed by the admissible value of the safety coefficient. The value of the yield strength determines the change of the

Table 2

Calculated values of forces acting on the pump gear and shafts

No.	V_g, cm^3	b, mm	P, kW	M_a, N·mm	F_d, N	F_{rx}, N	F_{x1}, N	F_{x2}, N	F_y, N	F_{R1}, N	F_{R2}, N
1	0.81	2.3	0.59	1794	138	838.35	700.35	976.35	58.57	703.8	841.8
2	0.99	2.8	0.74	2184	168	1020.6	852.6	1188.6	71.30	856.8	1024.8
3	1.2	3.4	0.93	2652	204	1239.3	1035.3	1443.3	86.58	1040.4	1244.4
4	1.7	4.8	1.35	3744	288	1749.6	1461.6	2037.6	122.23	1468.8	1756.8
5	2.19	6.2	1.78	4836	372	2259.9	1887.9	2631.9	157.88	1897.2	2269.2
6	2.62	7.4	2.15	5772	444	2697.3	2253.3	3141.3	188.43	2264.4	2708.4
7	3.18	9	2.64	7020	540	3280.5	2740.5	3820.5	229.18	2754	3294
8	3.54	10	2.97	7800	600	3645	3045	4245	254.64	3060	3660
9	4.25	12	3.60	9360	720	4374	3654	5094	305.57	3672	4392
10	4.71	13.3	3.99	10 374	798	4847.85	4049.85	5645.85	338.67	4069.8	4867.8
11	6.01	17	5.09	13 260	1020	6196.5	5176.5	7216.5	432.89	5202	6222
12	7.82	22.1	6.62	17 238	1326	8055.45	6729.45	9381.45	562.75	6762.6	8088.6

From the data presented in this table, we noticed a proportional increase by eight to ten times the calculated values between the first and the last parameterized model pump, having different sizes.

This methodology of calculation of forces is quite accurate, being the basis of the complex dimensioning approach of the spur gear pumps and it is used in industry.

4. FINITE ELEMENTS SIMULATION OF THE LOADS ON THE SPUR GEARS

By using the values of the gear and bearing forces and the pressure distribution forces, a FEM simulation model is created to validate the various variants of parameterized concept of the pump product. Following these simulations, important data are obtained and presented, concerning the distribution of the stresses and deformations that appeared within the pump assembly.

As a result, under absolute safety conditions for the operation of the pump assembly, it is required that the actual stresses resulted in the calculation should be lower than the critical ones.

model, of the restrictions and/or the loads, so that the deformations should remain, if possible, elastic, with a convenient safety coefficient [14].

The physical properties of the pump components' materials, especially the yield strength crucially affect the results of the simulations performed in this analysis.

The pump body is made of an aluminium alloy AlSi9Cu3(Fe), with the yield strength of $R_m=2.4\times10^8$ N/m^2, HBS 2.5/ 62.5=104, Si (9.75%), Fe (0.73%), Cu (3.04%), Mn (0.08%), Ni (0.43%), Zn (0.2%), Mg (0.3%), Sn (0.18%), Ti (0.18%) [3]. The pump cover is made of AlSi6Cu4, yield strength of $R_m=2\times10^8$ N/m^2, HBS 2.5/ 62.5=121 with the composition: Si (7.97%), Fe (0.53%), Cu (5.12%), Mn (0.12%), Ni (0.01%), Zn (0.12%), Mg (0.7%). These alloys are recommended for casting parts, having a very good machinability. For the gears and their shafts it was used a steel alloy of $R_m=3.5\times10^8$ N/m^2, HRC=51 and for the assembly elements (pins and screws) a quality carbon steel of $R_m=2.5\times10^8$ N/m^2.

The discretization of the main components is an important stage of the finite element analysis. A correct refining of the mesh leads to a reduced error of the calculation model, the values

indicated on the finite element structure being thus closer to the real ones [1], [15].

After the simulation are done, the gears' results will present a much lower error rate than the one of the other components, but all being within the accepted limits of good practice related to FEM analyses [6], [14].

Physical constraints are applied between the components of the gear pump, the significations, the application way, the choosing criteria, being presented at length in the works [1], [3], [15].

An important stage in the analysis of the assembly by FEM simulation is the application of virtual loads on certain surfaces belonging to the pump components.

They simulate the real loads that the model must bear during operation. Pressure and distributed force loads are applied to the pump assembly [7], [16].

Regarding the theoretical considerations, inside the pump assembly there are forces that act on the teeth, some pressures are radially distributed in the gaps between the teeth, other pressures act in the bearings, on the plane surfaces of the cover and of the compensator, in contact with the front surfaces of the gears.

The results of such loads determine the appearance of stresses and deformations inside the pump's assembly [15]. Pressures are applied to each gear, in the gaps between the teeth, but also in the inlet and outlet areas (Fig. 6), starting from a value of 1.4×10^6 N/m^2 to the value of 1.5×10^7 N/m^2 (150 bar), the nominal pressure for pump operation. The applied pressures will increase in radial distribution, the lowest value being found in the inlet chamber, while the highest value being in the outlet chamber [12]. Two forces of equal value but opposite direction F_d, also act tangentially on the gearing teeth, and such forces, together with the forces generated by the applied pressures (F_{rx1} and F_{rx2}), lead to the appearance of resulting forces F_{x1}, F_{x2} in the gearing teeth and in the gear shafts.

From the composition of these forces with the reaction force as a reaction of the gearing teeth, F_y, the resulting forces F_{R1} and F_{R2} (Fig. 5) are obtained, these forces stress the bearings of the driving and driven gears. Fig. 7 presents how the loading force took place on the teeth of the two gears that are in contact at a certain time. The pressures and the forces thus distributed lead to the creation of stresses in toothing, in the gear crown and in the gear shafts, but also in the compensator, body and cover as bearing supports. The analysis of such components show that the teeth are most stressed when they reach the area where maximum pressure is exerted on the flanks, but also in the gearing area [1], [5]. Based on the indicated values, deformations of such areas are also determined, the values are obtained through FEM analysis.

Following the specific calculations, we can determine by simulation the maximum and the minimum stresses values appeared in the main components of the pump, the deformations and the rates of error of such calculations [2] for

Table 3

Variation of maximum stresses, of deformations and of the error rates

No.	b, mm	F_d, N	Driving gear			Driven gear			Compensator		Body		Cover	
			Stress, $\times10^8$ N/m^2	Disp, $\times10^{-3}$ mm	Er, %	Stress, $\times10^8$ N/m^2	Disp, $\times10^{-3}$ mm	Er, %	Stress, $\times10^6$ N/m^2	Er, %	Stress, $\times10^6$ N/m^2	Er, %	Stress, $\times10^6$ N/m^2	Er, %
1	2.3	138	1.36	3.3	6.59	1.39	4.9	5.89	7.72	14.4	7.72	11.3	11.5	11.2
2	2.8	168	1.08	3.1	6.27	1.39	5.1	5.82	9.6	16.7	4.77	11.4	13	11
3	3.4	204	1.26	3.2	6.15	1.43	5.2	5.92	10.6	16.5	3.38	12.3	14.3	10.8
4	4.8	288	1.21	3.4	6.5	1.47	5.9	6.38	14.6	17.2	4.54	12.2	19.6	10.6
5	6.2	372	1.08	3.7	6.38	1.51	6.3	6.23	17.2	14.3	8.89	12.4	24.4	10.3
6	7.4	444	1.1	3.6	6.3	1.49	6.5	6.56	19.4	17.1	6.87	14.8	27.8	10.2
7	9	540	1.21	4	6.56	1.46	6.9	6.61	19.1	16.4	7.57	13.6	22.7	10.2
8	10	600	1.09	4.3	7	1.65	7.4	6.92	26.2	14.8	9.45	13	26.1	11.1
9	12	720	1.08	4.4	7.11	1.79	7.8	6.95	28.6	16.3	9.22	13.2	28.7	11.2
10	13.3	798	1.07	4.6	7.06	1.82	8.1	7.26	26.1	18.2	12	13.1	31.5	11.1
11	17	1020	1.3	5.2	7	1.98	9.5	7.21	39	16.3	14.1	12.4	39.9	11.7
12	22.1	1326	1.54	5.7	6.79	2.56	10.9	7.46	54.1	17.3	21	13.4	48.2	11.3

all 12 parameterized variants, according to Table 3.

Maximum stresses appear for the last parameterized model variant (width of gear teeth b=22.1 mm, tangential forces F_d=1326 N).

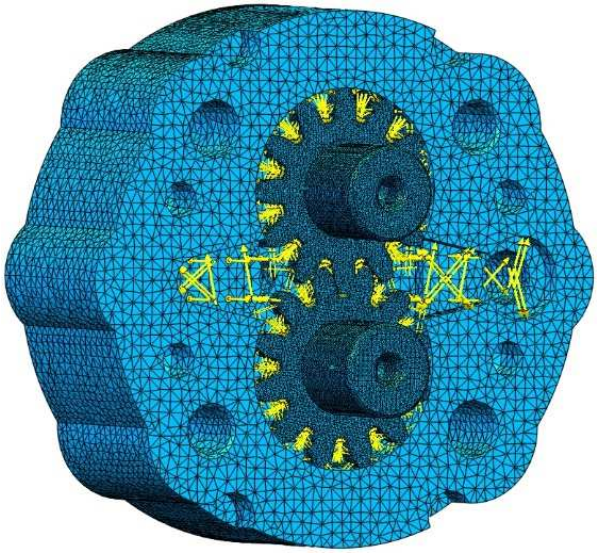

Fig. 6. Radial distribution of pressures inside the pump.

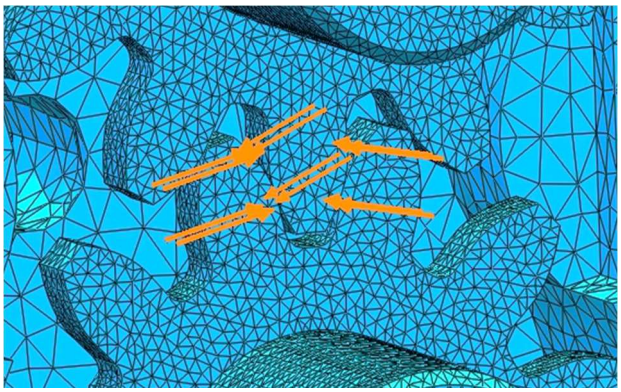

Fig. 7. Forces distribution on the teeth flanks.

The most stressed components are the gears teeth, of course, while the maximum stress (2.56×108 N/m2) occurs for the driven gear, being located in the teeth root, as also specified in [13]. The driving gear also presents maximum stress (1.54×108 N/m2), located at the root of the geared teeth. The compensator has a maximum stress of 54×106 N/m2, the body a maximum stress of 21×106 N/m2, while the cover a maximum stress of 48.2×106 N/m2.

The stress appears, as well, in the other pump components: pins, screws and gasket, but their values are very low and are not influencing its functioning.

According to Fig. 8, a., it is observed that the stress distribution is higher on the driven gear bearings (pump body and cover), in the gearing area (Fig. 8, b.) and in the area of maximum pressures created in the gaps of the teeth.

Of course, even for these components, it is out of the question to reach the value of yield strength (2.6×10^8 N/m^2) of the aluminum alloy that they are made of.

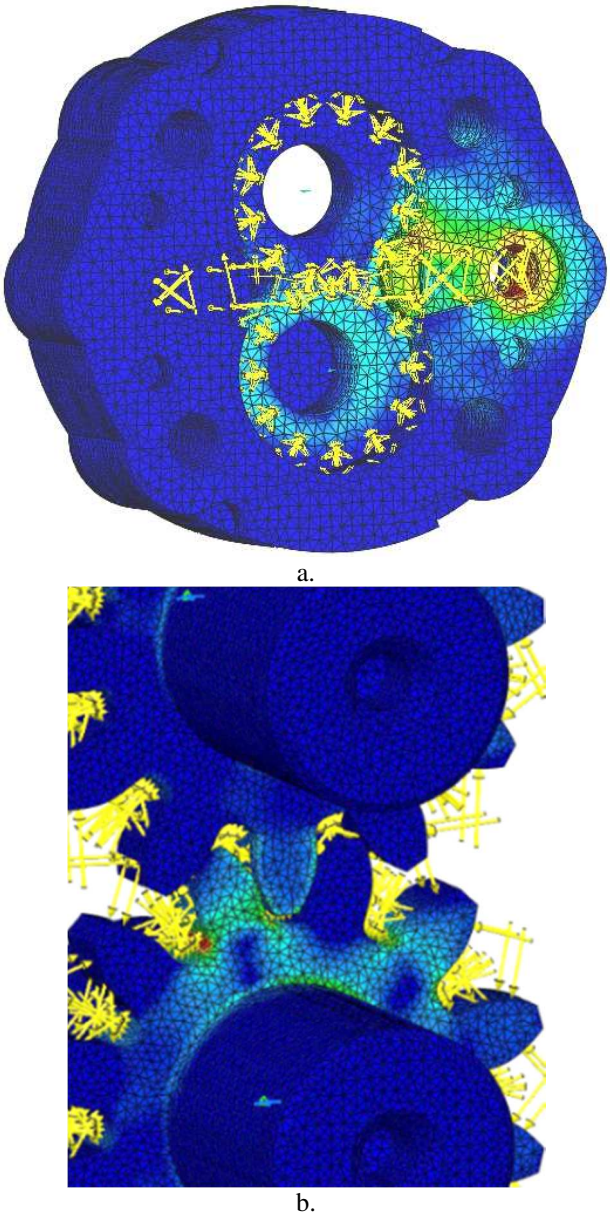

a. b.

Fig. 8. Von Mises stress representation of the main pump components: a. body and b. gears

Of the four representations (Fig. 6, 7 and 8) it can be drawn out how the pump components meshing has been prepared. The mesh of the finite elements is denser on gears, which leads to lower error percentages.

According to Fig. 9, it is observed that the stress distribution is higher on the driven gear bearings (compensator and cover), in the gearing area and/or in the area of maximum pressures created in the gaps of the teeth.

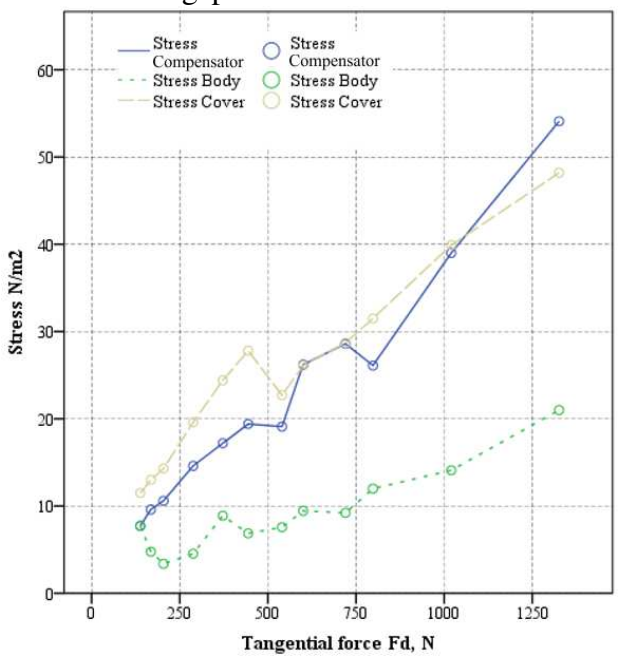

Fig. 9. Stress evolution in the body, cover and compensator, depending on applied F_d forces

Fig. 10 graphically present the progress of the stresses that occurred in the driving and driven gears, respectively, according to the values of F_d forces applied on the teeth.

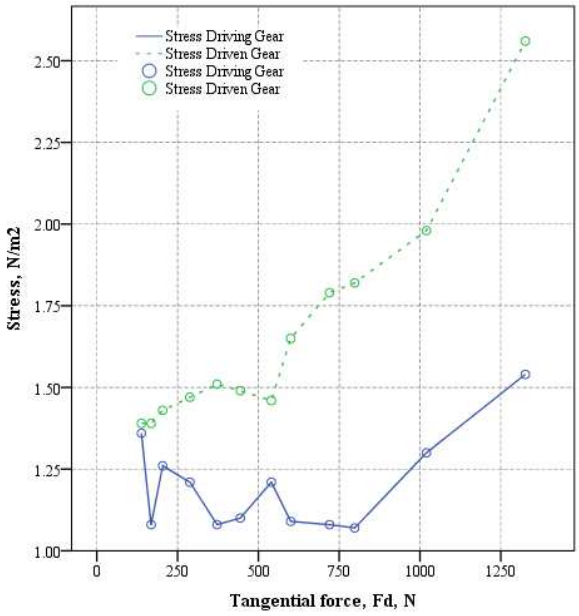

Fig. 10. Stress evolution in the two gears, depending on the applied F_d forces

Fig. 11 shows the displacements in both gears of the analyzed pump for the third parameterized model variant (Tab. 3). We can observe the areas where the stress increases, as well the pressures distribution between the gears teeth.

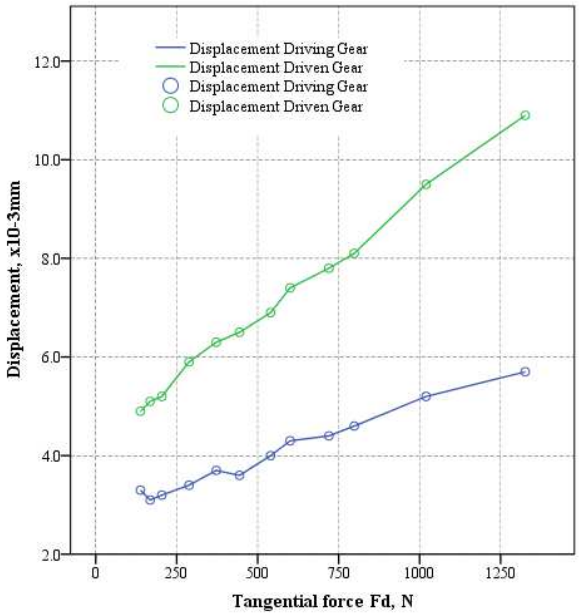

Fig. 11. Displacement evolution in gears depending on applied F_d force for the third pump variant

Resuming of the calculation steps in this study was performed by many iterations, required to achieve the objectives imposed by the authors regarding the low error percentage. The simulations were performed on a personal computer with processor Intel Core i7-4702MQ 2,2GHz and 16 GB RAM, operating system Windows 8.1 Pro 64-bit. The average time for each FEM simulation was about 2 hours and there were used 516877 nodes and 620937 finite elements arranged on all the components of the pump assembly with 1550631 degrees of freedom, on a high meshing of the assembly.

5. CONCLUSIONS

The parametric design studies, fast creation of several constructive variants of the same product, finite element analysis for each of these options prove to be useful tools for the simulation design of mechanical products.

Thus, it is possible to provide a preliminary validation of the product, which is an important stage in product design optimization [2].

The analysis performed on the parametric model alternative solutions of the pump assembly provided the theoretical validation of all 12 identified solutions, as the maximum stress values present in the components being lower than the yield strength of their materials.

After an optimum re-modelling of the pump assembly corresponding to the alternative third solution, already in production, weight decrease from 587g to 546g. Reducing the pump weight, but maintaining an imposed flow value is important for the production process due to the possibility of increasing the production's efficiency and reducing the manufacturing price of any of the pump variant.

The analysis presented in this paper does not take into account the pressure pulsation and an increase of the hydraulic fluid temperature in the functioning time. A future research will consist in a verification of the obtained prototype variants in experimentally conditions measuring the real stress values, flows, noise and vibrations. This phase will be, in fact, the final test before a series production.

ACKNOWLEDGEMENT

The work has been funded by the Sectorial Operational Programme Human Resources Development 2007-2013 of the Ministry of European Funds through the Financial Agreement POSDRU/159/ 1.5/S/138963.

The authors wish to thank HESPER Bucharest and MEFIN Sinaia companies for pump and tests.

6. REFERENCES

[1] Houzeaux, G., Codina, R., *A finite element method for the solution of rotary pumps*. Computers & Fluids, Vol. 36, No. 4, 2007.

[2] Ghionea, I., G., *Researches on optimization by simulation of the industrial products design*. Phd. Thesis, University Politehnica of Bucharest, Romania, 2010.

[3] Athanassios, M., Pupăză, C., *Design optimization of high ratio planetary systems. Power transmissions*. In: Proceedings of the 4th International Conference. Mechanisms and Machine Science 13, Springer Science, pp. 479-485, ISBN 978-94-007-6557-3, 2012, Sinaia, Romania.

[4] Kollek, W., Osiński, P., *Modelling and design of gear pumps*, Wroclaw University of Technology Publishing House, ISBN 978-83-7493-452-7, Wroclaw, Poland, 2012.

[5] Faggioni, M., Samani, F., S., Bertacchi, G., Pellicano, F., *Dynamic optimization of spur gears*. Mechanism and Machine Theory, Vol. 46, pp. 544–557, 2011.

[6] Mucchi, E., Dalpiaz, G., *Experimental validation of a model for the dynamic analysis of gear pumps*. Proceedings of 25th International Conference on Design Theory and Methodology, Oregon, USA, 2013.

[7] Linke, H., Hantschack, F., Trempler, U., *New results on the calculation of the load capacity of internal gears*. Proceedings of International Conference on Gears. Society for Product and Process Design. pp. 741-753, ISBN 978-3-18-092108-2, 2010, Technical University of Munich, Germany.

[8] SR ISO 53:2011, SR ISO 701:2011, SR ISO 677:2011, Standards on gears, 2011.

[9] Osiński, P., *Modelling and design of gear pumps with modified tooth profile*, Lambert Academic Publishing, ISBN 978-365-952-662-6, Saarbrucken, Germany, 2014.

[10] Prodan, D., *Hydraulics. Elements, Subsystems, Systems*. Printech, ISBN 973-652-677-1, Bucharest, Romania, 2002.

[11] Product Catalogue Hesper. *Gear pumps*.

[12] Vasiliu, N., Vasiliu, D., *Hydraulic and pneumatic actuations*, Vol. I. Technic Publishing House, ISBN 973-31-2248-3, Bucharest, Romania, 2005.

[13] Shanmugasundaram, S., Maasanamuthu, S., Muthusamy, N., *Profile modification for increasing the tooth strength in spur gear using CAD*. Engineering Design SCIRP, pp. 740-749, ISSN 1947-3931, 2010.

[14] Mucchi, E., Rivola, A., Dalpiaz, G., *Modelling dynamic behaviour and noise generation in gear pumps: procedure and validation. Applied Acoustics*, Vol. 77, 2014.

[15] Casoli, P., Vacca, A., Franzoni, G., *A numerical model for the simulation of external gear pumps*. Proceedings of the 6th International Symposium on Fluid Power

JFPS, ISBN 4-931070-06-x, Tsukuba, Japan, 2005.

[16] Opran, C., Ghionea, I., Pricop, M., *Embedded modelling and simulation software system for adaptive engineering of hydraulic gear pumps*, Proceedings of the 26th DAAAM International Symposium, pp.0311-0319, DAAAM International, ISBN 978-3-902734-07-5, Vienna, Austria, 2015.

Proiectarea parametrică asistată de calculator a pompelor hidraulice cu roţi dinţate

Rezumat : Această lucrare abordează o metodologie de proiectare a pompelor hidraulice cu roți dințate cilindrice. Pe baza cerințelor impuse de către un producător român de pompe, obiectivul general al acestei cercetări este acela de a identifica mai multe alternative de proiectare a acestora și de a propune soluții constructive îmbunătățite. Abordarea este susținută de validare matematică și simulare FEM pentru diferite variante modelate 3D, scopul fiind obținerea unei game mai largi de debite. Folosind programele CATIA și Visual Basic, strategia propusă prezintă rezultatele care sintetizează valorile maxime de stres, deformarea și eroarea de calcul procentual pentru fiecare soluție găsită.

Ionuţ Gabriel GHIONEA, Phd. Eng., Lecturer, University Politehnica of Bucharest, Faculty of Engineering and Management of Technological Systems, Department of Machine Manufacturing Technology, E-mail: ionut76@hotmail.com, Office Phone: +4021 402 9373, Address: Bucharest, Romania, Spl. Independenţei nr. 313, district 6.

Nicolae IONESCU, Phd. Eng., Professor, University Politehnica of Bucharest, Faculty of Engineering and Management of Technological Systems, Department of Machine Manufacturing Technology, E-mail: ionescu_upb@yahoo.com, Office Phone: +4021 402 9373, Address: Bucharest, Romania, Spl. Independenţei nr. 313, district 6.

Adrian GHIONEA, Phd. Eng., Dr.H.C., Professor, University Politehnica of Bucharest, Faculty of Engineering and Management of Technological Systems, Department of Machines and Manufacturing Systems, E-mail: adrianghionea@yahoo.com, Office Phone: +4021 402 9420, Address: Bucharest, Romania, Spl. Independenţei nr. 313, district 6.

Saša ĆUKOVIĆ, PhD, Scientific Associate, University of Kragujevac, Faculty of Engineering, Sestre Janjic 6, 34000 Kragujevac, cukovic@kg.ac.rs, Phone: +38134335990, ext. 643, Address: Sestre Janjic 6, 34000 Kragujevac, Serbia.

Sergiu TONOIU, Phd. Eng., Professor, University Politehnica of Bucharest, Faculty of Engineering and Management of Technological Systems, Department of Machine Manufacturing Technology, E-mail: sergiu_ton@yahoo.com, Office Phone: +4021 402 9373, Address: Bucharest, Romania, Spl. Independenţei nr. 313, district 6.

Mădălin CATANĂ, Phd. Eng., Associate Professor, University Politehnica of Bucharest, Faculty of Engineering and Management of Technological Systems, Department of Machine Manufacturing Technology, E-mail: mg_catana@yahoo.com, Office Phone: +4021 402 9373, Address: Bucharest, Romania, Spl. Independenţei nr. 313, district 6.

Iqbal JAMSHED, Phd. Eng., Associate Professor, FAST National University of Computer and Emerging Sciences, Department of Electrical Engineering, E-mail: jamshed.iqbal@nu.edu.pk, Office Phone: +92 324 5229326, Address: A.K. Brohi Road, H-11/4, Islamabad, Pakistan.